Active negative-index metamaterial powered by an electron beam

M. A. Shapiro,[1] S. Trendafilov,[2] Y. Urzhumov,[3] A. Alù,[4] R. J. Temkin,[1] and G. Shvets[2,*]

[1]*Plasma Science and Fusion Center, Massachusetts Institute of Technology, Cambridge, Massachusetts 02139, USA*

[2]*Department of Physics, The University of Texas at Austin, Austin Texas 78712, USA*

[3]*Center for Metamaterials and Integrated Plasmonics, Pratt School of Engineering, Duke University, Durham, North Carolina 27708, USA*

[4]*Department of Electrical and Computer Engineering, The University of Texas at Austin, Austin Texas 78712, USA*

(Received 23 December 2011; published 21 August 2012)

An active negative index metamaterial that derives its gain from an electron beam is introduced. The metamaterial consists of a stack of equidistant parallel metal plates perforated by a periodic array of holes shaped as complementary split-ring resonators. It is shown that this structure supports a negative-index transverse magnetic electromagnetic mode that can resonantly interact with a relativistic electron beam. Such a metamaterial can be used as a coherent radiation source or a particle accelerator.

DOI: 10.1103/PhysRevB.86.085132 PACS number(s): 81.05.Xj, 07.57.Hm, 41.60.Bq, 41.75.Lx

I. INTRODUCTION

Artificially structured metamaterials (MTMs) possess exotic macroscopic electromagnetic properties that cannot be achieved in natural materials. Constructed from simple planar elements such as split-ring resonators and thin wires,[1] MTMs enable a variety of applications such as "perfect" lenses, compact transmission lines and antennas, electromagnetic cloaks, and many others.[2–5] The negative refractive index[1,6–8] is one of the most surprising and thoroughly studied properties enabled by MTMs. In this article we describe a new class of negative-index MTMs that can strongly interact with an electron beam, thereby opening new opportunities for vacuum electronics devices such as coherent radiation sources and particle accelerators. The specific implementation of such a negative-index metawaveguide (NIMW) analyzed in this paper and schematically shown in Fig. 1 is obtained by patterning an array of split-ring resonator cutouts on the plates of a stack of planar metallic waveguides.

The NIMW belongs to the category of complementary metamaterials (C-MTMs).[9] C-MTMs utilize the complements of the traditional split-ring resonators (SRR) in order to achieve a complementary electromagnetic response: an SRR exhibits a strong magnetic response while a C-SRR has a strong electric response. Narrow waveguides patterned with C-SRRs have been used[10] to demonstrate enhanced tunneling of transverse electromagnetic (TEM-like) waves, as well as for making a negative index metamaterial for wave propagation normal to the metal screens.[11] In this paper, we demonstrate that this structure supports a negative-index transverse magnetic (TM) mode: an electromagnetic mode propagating in the x direction, with E_x being the only nonvanishing component in the waveguide's mid-plane at $z = 0$. As demonstrated below, the negative effective permittivity of the NIMW $\epsilon_{\rm eff} < 0$ is imparted to it by resonant C-SRRs,[9,10] while the negative effective permeability $\mu_{\rm eff} < 0$ is due to the transverse confinement of the TM modes[12] supported by the narrow (width d in the z direction is much smaller than the wavelength $\lambda \equiv 2\pi c/\omega$) waveguides formed by the neighboring plates. The importance of utilizing TM modes lies in their ability to resonantly interact via finite E_x with relativistic electron beams when their phase velocity $v_{\rm ph} \equiv \omega/k_x$ is equal to the beam's velocity v_b. Such an interaction can be exploited to either transfer the electromagnetic energy to the beam (particle accelerator) or to extract energy from the beam (coherent radiation source).

The attraction of the NIMW for coherent high-frequency radiation generation is threefold. First, the opposite sign of the group velocity and the beam velocity can result in an instability utilized in backward-wave oscillators (BWO) or (for lower beam currents) amplifiers (BWA).[13] The subwavelength nature (lateral period $b \ll \lambda$) of the NIMW supported by its resonant C-SRRs distinguishes it from the traditional BWOs, which rely on the interaction between an electron beam and a spatial harmonic of the electromagnetic field in a periodic structure. Second, the low group velocity $v_g \ll c$ of the negative-index waves due to the NIMW's resonant C-SRRs increases spatial gain, reduces the starting current requirement of a BWO, and enables shorter structures. Third, NIMW's constitutive elements (C-SRRs) can be produced using standard planar fabrication techniques. This is particularly advantageous for the generation of THz and millimeter waves (corresponding to frequencies between 0.3 and 3 THz) because the fabrication of conventional BWOs[14] relies on high-precision machining that becomes challenging for shorter wavelengths.

Because the metallic planes of the NIMW are *parallel* to the direction of the beam's velocity, they do not obstruct the beam's propagation in the same way as, for example, multilayer fishnet metamaterials[7,15–17] containing small openings through which the beam must propagate normally to the metal surface. The interaction between the beam and the NIMW is further facilitated by the spatial distribution of the longitudinal electric field E_x, which is maximized at the beam's location as shown in Figs. 1(a) and 1(c). This favorably compares with multilayer fishnet structures which have a very small and highly nonuniform[15–17] longitudinal electric field inside the hole. Also, the output radiation frequency of a NIMW can be accurately and rapidly controlled by electric or optical tuning of the resonant frequency of the C-SRRs.[18] Finally, unlike the negative index multilayer fishnet structures which have subwavelength dimensions only along one direction, all dimensions of a NIMW (see caption of Fig. 1) can be made strongly subwavelength, thereby making it a genuine metamaterial. We note that the absolute instability of electron beams inside a negative-index medium has been suggested

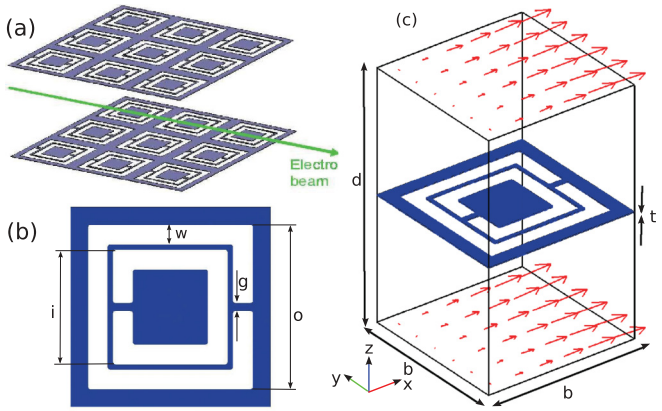

FIG. 1. (Color online) (a) Schematic of a negative-index metawaveguide (NIMW) composed of a stack of metal plates patterned by complementary split-ring resonators (C-SRRs). An electron beam propagating in the x direction and interacting with the NIMW is also shown. (b) C-SRR's dimensions: outer ring slot length, $o = 6.6$ mm; inner ring slot length, $i = 4.6$ mm; slot width, $w = 0.8$ mm; gap width, $g = 0.3$ mm. (c) Single cell of a NIMW and midplane electric fields (arrows) interacting with the beam: stacking distance between metal planes, $d = 12.8$ mm; square lattice period, $b = 8$ mm; metal thickness, $t = 0.05$ mm. These dimensions were chosen for a frequency near $f_0 = 5$ GHz as described in detail below.

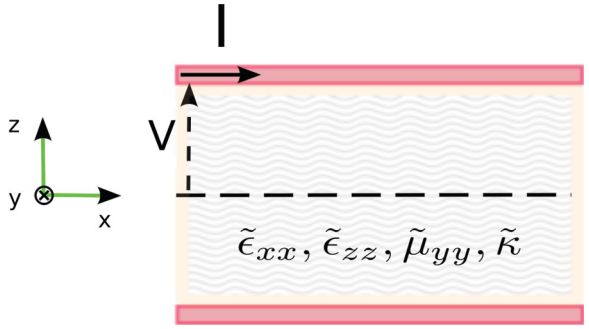

FIG. 2. (Color online) Side view of a parallel plate waveguide with effective filler medium. Voltage V and current I are used for extracting the MTM's constitutive parameters.

earlier,[19] albeit limited to a hypothetical isotropic negative index material.

The rest of the manuscript is organized as follows. An analytic homogenization theory of an active beam-powered NIMW is developed in Sec. II. The results of numerical simulations using the COMSOL MULTIPHYSICS[20] finite-element-method (FEM) code are presented in Sec. III. Section IV concludes and suggests possible practical applications.

II. ANALYTIC MODEL OF A NEGATIVE INDEX METAWAVEGUIDE

Below we demonstrate that the NIMW shown in Fig. 1 can be properly described as an effective bianisotropic[21] negative index medium for electromagnetic waves propagating in the x direction. By restricting the macroscopic (i.e., properly averaged over the metamaterial's unit cell) electromagnetic field components to $\bar{E}_z$ and $\bar{H}_y$, such a metamaterial can be characterized by a set of constitutive parameters ϵ_{eff}, μ_{eff}, and the bianisotropy coefficient κ_{eff} defined according to

$$\bar{D}_z = \epsilon_{\text{eff}} \bar{E}_z - i\kappa_{\text{eff}} \bar{H}_y, \quad \bar{B}_y = +i\kappa_{\text{eff}} \bar{E}_z + \mu_{\text{eff}} \bar{H}_y \qquad (1)$$

and can be shown[21,22] to support electromagnetic waves propagating with refractive index n given by

$$n \equiv \frac{ck_x}{\omega} = \pm\sqrt{\epsilon_{\text{eff}}\mu_{\text{eff}} - \kappa_{\text{eff}}^2}, \qquad (2)$$

where the negative sign is assigned to the propagating waves with $\epsilon_{\text{eff}}, \mu_{\text{eff}} < 0$.

To understand the emergence of negative-index waves in a NIMW, we, first, examine the origin of $\mu_{\text{eff}} < 0$ for wave propagation through a metamaterial composed of an array of planar waveguides with perfectly electrically conducting (PEC) walls stacked along the z direction. It is well established that a metamaterial composed from an array of metallic plates may be rigorously homogenized by studying the modes excited between any two neighboring plates.[23,24] Here we apply this homogenization model to the parallel-plate metamaterial of Fig. 1(a). A homogenized representation of the metamaterial is shown in Fig. 2. The effective metamaterial properties are determined by the dominant TM mode, with wave number k_x and frequency ω. We note that the longitudinal component of the electric field, enabled by the parallel plates, can resonantly interact with an electron beam propagating in the x direction. The TM_1 mode is symmetric with respect to the $z = 0$ midplane and possesses nonvanishing fields E_x (even function of z), E_z, and H_y (both odd functions of z). The subscript 1 refers to the number of nodes of the transverse field components E_z and H_y along the z direction.

Note that while the PEC assumption is valid for THz and millimeter waves, it starts breaking down for frequencies exceeding tens of THz (mid-IR part of the spectrum) because of the increasing penetration of the field into the metal.[25] Such high frequencies are outside of the scope of this paper. We also note that similar structures have been proposed[11] for negative index propagation perpendicular to C-SRR patterned metal screens. Such propagation geometry does not lend itself to effective beam-structure interaction because the beam would have to propagate through very narrow slits.

In anticipation of the need to emulate the effects of C-SRRs and the electron beam, the waveguide is assumed to be filled with a material characterized by a permittivity tensor with nontrivial components $\tilde{\epsilon}_{xx}$ and $\tilde{\epsilon}_{zz}$ and a single nonvanishing component $\tilde{\kappa}$ defined as in Eq. (1). Finite $\tilde{\kappa}$ emulates magneto-optical coupling introduced by the C-SRR,[21] $\tilde{\epsilon}_{zz} \neq 1$ emulates resonant electric response of the C-SRR, while $\tilde{\epsilon}_{xx} \neq 1$ emulates the wave's interaction with an electron beam when the resonance condition $\omega = k_x v_b$ is satisfied. The metamaterial becomes active when $\text{Im}(\tilde{\epsilon}_{xx}) < 0$. This anisotropic gain due to the beam-structure interaction should be contrasted with the isotropic gain obtained from more standard gain media, such as quantum dots or organic dies, used for loss compensation.[26]

The effective constitutive parameters may be computed by analyzing the propagation properties of the dominant TM_1 mode, using the transmission-line characteristic impedances for forward- and backward-propagating TM waves according to $Z_{\text{ch}}^{\pm} \equiv \pm V/I$, where the transmission line's voltage V and

current I are defined according to

$$I = -\int_{-b/2}^{b/2} dy H_y(x = \mp b/2, z = t/2),$$
$$V = \frac{1}{b}\int_{-b/2}^{b/2} dy \int_{t/2}^{d/2} dz E_z(x = \mp b/2), \tag{3}$$

and the top and bottom signs correspond to the forward and backward waves, respectively. While $Z_{\rm ch}^{+} = Z_{\rm ch}^{-}$ for an air filled transmission line shown in Fig. 2, that would no longer be the case when magnetoelectric coupling is present in the filling medium, as would be the case in the more general bianisotropic structure shown in Fig. 1. Effective material parameters can then be obtained from the transmission-line model through

$$\epsilon_{\rm eff} = \frac{ck_x}{\omega}\frac{2}{Z_{\rm ch}^{+} + Z_{\rm ch}^{-}} Z_0,$$
$$\mu_{\rm eff} = \frac{ck_x}{\omega}\frac{2}{Y_{\rm ch}^{+} + Y_{\rm ch}^{-}}\frac{1}{Z_0}, \tag{4}$$
$$\kappa_{\rm eff} = i\frac{Y_{\rm ch}^{+} - Y_{\rm ch}^{-}}{2} Z_0 \mu_{\rm eff},$$

where $Z_0 = 377\ \Omega$ is the free-space impedance and $Y_{\rm ch} \equiv 1/Z_{\rm ch}$ is the characteristic admittance of the transmission line.

Applying the above definitions of effective parameters and characteristic impedances to the $\rm TM_1$ mode of the conventional parallel-plate metamaterial in Fig. 2 made of smooth metallic plates and suitable filler medium, we obtain $\kappa_{\rm eff} = \tilde{\kappa}$ and

$$\epsilon_{\rm eff} = \tilde{\epsilon}_{zz}\frac{\pi b}{d}, \quad \mu_{\rm eff} = \left[\tilde{\mu}_{yy} - \left(\frac{\pi/d}{\omega/c}\right)^2 \frac{1}{\tilde{\epsilon}_{xx}}\right]\frac{d}{\pi b}, \tag{5}$$

resulting in the dispersion relation for the $\rm TM_1$ wave,

$$\frac{ck_x}{\omega} = \pm\sqrt{\tilde{\epsilon}_{zz}\tilde{\mu}_{yy} - \tilde{\kappa}^2 - \left(\frac{\pi/d}{\omega/c}\right)^2 \frac{\tilde{\epsilon}_{zz}}{\tilde{\epsilon}_{xx}}}. \tag{6}$$

Several insights can be gained from Eq. (5). First, the effective magnetic permeability turns negative for $\omega < \omega_c$, where $\omega_c = c\pi/d$ is the cutoff frequency of the considered $\rm TM_1$ mode. Therefore, one approach to achieving negative-index propagation at $\omega < \omega_c$ is to pattern the waveguide's wall in such a way as to ensure that $\tilde{\epsilon}_{zz}(\omega) < 0$. Second, if $\mathrm{Im}(\tilde{\epsilon}_{xx}) \neq 0$ (as is the case for a beam resonantly interacting with the E_x component of the mode), then $\mathrm{Im}(\mu_{\rm eff}) \neq 0$, resulting in an active (gain) metamaterial. That the longitudinal component of the electric field E_x (and, therefore, $\tilde{\epsilon}_{xx}$) contributes to the effective magnetic permeability $\mu_{\rm eff}$ of confined TM modes has been known[8,12] from theoretical and experimental studies, but the possibility of employing an electron beam for controlling the imaginary part of $\mu_{\rm eff}$ and realizing gain in metamaterials has not been recognized. Finally, Eq. (6) can be recast in the conventional form for the theory of traveling wave tubes (TWTs)[13] by assuming that the waveguide is filled with an active medium with permittivity $\tilde{\epsilon}_{xx}^{(b)} = 1 - \omega_b^2/(\omega - k_x v_b)^2$, where ω_b is the electron beam plasma frequency. The resulting dispersion relation for the active NIMW can now be rewritten as

$$\left[k_x^2 - \frac{\omega^2}{c^2}\left(\epsilon_{\rm eff}\mu_{\rm eff} - \kappa_{\rm eff}^2\right)\right](\omega - k_x v_b)^2$$
$$= \frac{\omega^2}{c^2}(\mu_{\rm eff} - 1)\epsilon_{\rm eff}\omega_b^2, \tag{7}$$

where, because of the wave-beam interaction, the frequency ω is a complex number for a real propagation constant k_x. Analogous to the linear theory of the TWT,[13] Eq. (7) is quartic in ω having four complex roots that represent three forward waves (with positive, negative, and zero gain) and one backward wave (not affected by the beam). The maximum gain $\gamma_{\rm max} = \sqrt{3}/2\rho$ is achieved at the beam-wave synchronism $\omega_{\rm NIMW}(k_x) = k_x v_b$ (zero detuning) condition, where $\omega_{\rm NIMW}(k_x)$ is the dispersion relation without the beam, and the Pierce parameter[13] of the NIMW is given by

$$\rho = \left[\frac{1}{2}\frac{v_b^2}{c^2}(\mu_{\rm eff} - 1)\epsilon_{\rm eff}\omega_{\rm NIMW}\omega_b^2\right]^{\frac{1}{3}}. \tag{8}$$

III. NUMERICAL SIMULATIONS

After gaining significant physical insights from analytic modeling of a smooth-walled structure, we proceed to extract the constitutive parameters of the NIMW with unit cell shown in Fig. 1 through first-principles electromagnetic simulations using COMSOL MULTIPHYSICS.[20] Periodic boundary conditions along the y and z directions are used, and a finite per-cell phase shift $\Phi_x \equiv k_x b$ is assumed in the x direction. While the present design is for microwave frequencies ($f \approx f_0 = 5$ GHz; physical dimensions are given in Fig. 1), it can be scaled down to mm-wave/THz frequencies. The dispersion relations of the lowest-order modes are shown in Fig. 3(a). A narrow-band negative index (NI) $\rm TM_1$-like mode is indeed found in the $5.33\ \mathrm{GHz} < f < 5.65$ GHz frequency range located below the cutoff frequency $f_c \equiv \omega_c/2\pi \approx 11.7$ GHz. As was remarked earlier[16] in the context of multilayer fishnet structures, complex three-dimensional metamaterials rarely support pure TE or TM eigenmodes. The exact eigenmode of the NIMW is a mixture of the two, with the TM component dominating.

Note that a second subcutoff $\rm TM_1$-like mode with positive refractive index is also supported by the structure. The positive index (PI) mode's propagation is due to a higher-order *magnetic* resonance of the C-SRR around 11 GHz. This resonance strongly affects $\tilde{\mu}_{yy}$ that enters Eq. (5) ($\tilde{\mu}_{yy} \approx 1$ is assumed for the NI mode) and enables $\mu_{\rm eff} > 0$ for $f > 8.5$ GHz. Detailed discussion of the PI mode is outside of the scope of this paper, and we concentrate below on the NI mode.

The mode-specific effective parameters of the NI mode were extracted by applying Eqs. (3) and (4) to COMSOL-produced electromagnetic field profiles and plotted in Fig. 3(b) for moderate phase advances. We note that $\mu_{\rm eff}$ remains relatively flat, consistent with our original conjecture that the transverse confinement of the mode is responsible for its effective negative permeability. On the other hand, $\epsilon_{\rm eff}$ displays strongly dispersive behavior, consistent with its origin stemming from the resonant C-SRR element. We further

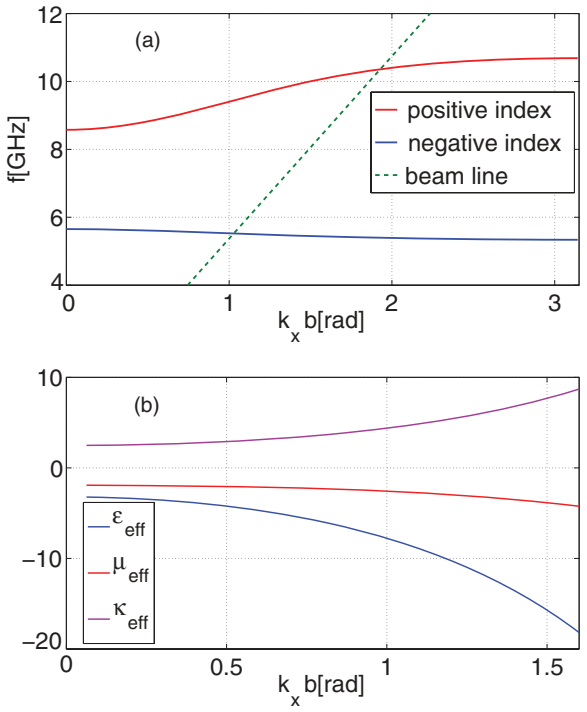

FIG. 3. (Color online) Modes of the NIMW calculated from COMSOL simulations. (a) Dispersion relation for the lowest TM_1-like modes (solid lines) and the "beam mode" (dashed line) defined by $\omega = k_x v_b$, where $v_b = 0.9c$. (b) Extracted effective parameters of the negative index mode.

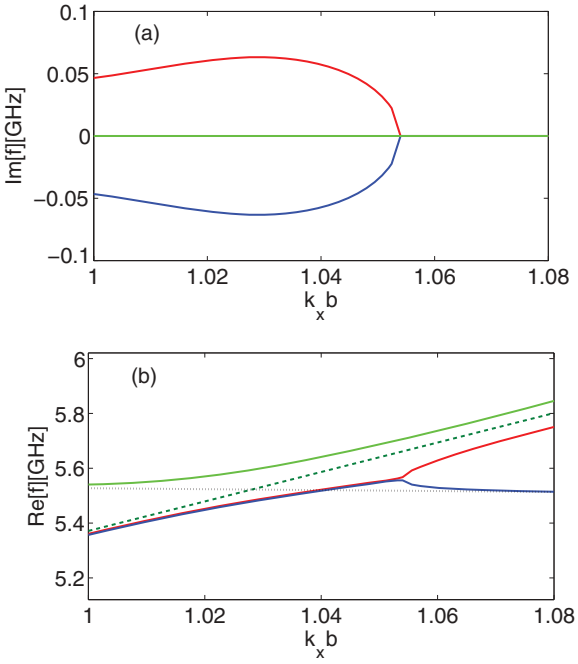

FIG. 4. (Color online) Dispersion characteristics of the active negative index TM_1-like wave in a NIMW coupled to an electron beam. NIMW parameters: same as in Fig. 1. Beam parameters are given in the text. (a) Imaginary and (b) real parts of the frequency as a function of the per-cell phase shift for three hybridized modes: growing, decaying, and neutral. Dotted/dashed lines: dispersion characteristics of the uncoupled NIMW/beam modes. All curves are plotted in the vicinity of the synchronous beam-mode interaction point defined by $\mathrm{Re}[\omega] = k_x v_b$.

observe that the bianisotropy coefficient κ_{eff} is rather large and, consistent with Eq. (2), explains why both ϵ_{eff} and μ_{eff} are nonvanishing (negative) at the $k_x = 0$ (cutoff) point, where $\epsilon_{\mathrm{eff}}\mu_{\mathrm{eff}} = \kappa_{\mathrm{eff}}^2$ is satisfied.

To examine the possibility of creating an active negative index metamaterial using a high-current electron beam coupled into the NIMW and to confirm the analytical predictions of Eqs. (7) and (8), we have carried out COMSOL simulations of the NIMW structure containing an electron beam in the middle of the unit cell. The beam's presence was modelled by assigning $\tilde{\epsilon}_{xx}^{(b)}$ to the region occupied by the beam and by assuming the following beam parameters: $v_b = 0.9c$, beam plasma frequency $\omega_b = 0.01(2\pi f_0)$, and the beam's radius $R = d/4$. The resulting complex ω, plotted as a function of the phase advance across the cell, is shown in Fig. 4 for phase advances in the vicinity of the beam-mode synchronism condition.

Three distinct complex ω's are found for each value of k_x. Modal degeneracies can be classified according to the value of the detuning parameter $\nu \equiv \omega_{\mathrm{NIMW}} - k_x v_b$. For $\nu > -3\rho/\sqrt[3]{4}$ two "slow" modes with $\mathrm{Re}[\omega]/k_x < v_b$ degenerate in $\mathrm{Re}[\omega]$ are found, one of them exponentially growing and the other one decaying. The third, "fast," mode with $\mathrm{Re}[\omega]/k_x > v_b$ is neutral (neither growing nor decaying) for $\nu > 0$. For $\nu < -3\rho/\sqrt[3]{4}$ all three modes (two "slow" and one "fast") become neutral and nondegenerate in $\mathrm{Re}[\omega]$. These numerical COMSOL results compare very well with the analytical predictions of Eq. (7) obtained by adjusting the effective beam plasma frequency to $\omega_b^{\mathrm{eff}} = 0.05\omega_b$ to account for only partial overlap between the beam and the negative-index TM mode. This reduction in ω_b^{eff} is associated with small shunt impedance of the resonant NIMW, which concentrates the electric energy away from the beam in the vicinity of the C-SRR. While ohmic losses reduce the growth rate, the instability still persists for somewhat higher beam densities corresponding to $\omega_b = 0.03(2\pi f_0)$.

IV. CONCLUSIONS

In conclusion, we have demonstrated a geometry to realize an active beam-driven negative index metawaveguide (NIMW) that supports transverse magnetic (TM) waves capable of resonantly interacting with an electron beam. A number of novel vacuum electronics devices that require backward waves and small group velocity, such as backward-wave oscillators and amplifiers, can be envisioned based on this concept. The subwavelength nature of the unit cell enables strong interaction with electron beams at the fundamental harmonic of the structure, while the resonant nature of the constitutive elements (complementary split-ring resonators) enables low group velocity and, potentially, agile frequency tuning.

One of the important issues not addressed in this paper is the ability of the C-SRR structure to withstand high radiation power. If radio-frequency breakdown can be avoided, then the narrow bandwith and small group velocity of NIMW could make it a potentially attractive structure for advanced

accelerator application. Breakdown in extremely narrow radio-frequency structures is presently the subject of active research (see, for example, Ref. 27 and references therein) and will be addressed in future publications.

ACKNOWLEDGMENTS

This work is supported by the U.S. DOE Grants No. DE-FG02-04ER41321 and No. DE-FG02-91ER40648.

*gena@physics.utexas.edu

[1]D. R. Smith, W. J. Padilla, D. C. Vier, S. C. Nemat-Nasser, and S. Schultz, Phys. Rev. Lett. **84**, 4184 (2000).
[2]J. B. Pendry, Phys. Rev. Lett. **85**, 3966 (2000).
[3]Y. Horii, C. Caloz, and T. Itoh, IEEE Trans. Microwave Theory Tech. **53**, 1527 (2005).
[4]R. W. Ziolkowski and A. Erentok, IEEE Trans. Antennas Propag. **54**, 2113 (2006).
[5]D. Schurig, J. J. Mock, B. J. Justice, S. A. Cummer, J. B. Pendry, A. F. Starr, and D. R. Smith, Science **314**, 977 (2006).
[6]V. G. Veselago, Sov. Phys. Usp. **10**, 509 (1968).
[7]J. Valentine, S. Zhang, T. Zentgraf, E. Ulin-Avila, D. A. Genov, G. Bartal, and X. Zhang, Nature **455**, 376 (2008).
[8]H. J. Lezec, J. A. Dionne, and H. A. Atwater, Science **316**, 430 (2007).
[9]F. Falcone, T. Lopetegi, M. A. G. Laso, J. D. Baena, J. Bonache, M. Beruete, R. Marques, F. Martin, and M. Sorolla, Phys. Rev. Lett. **93**, 197401 (2004).
[10]R. Liu, Q. Cheng, T. Hand, J. J. Mock, T. J. Cui, S. A. Cummer, and D. R. Smith, Phys. Rev. Lett. **100**, 023903 (2008).
[11]M. Beruete, M. Aznabet, M. Navarro-Cia, O. El Mrabet, F. Falcone, N. Aknin, M. Essaaidi, and M. Sorolla, Opt. Express **17**, 1274 (2009).
[12]G. Shvets, Phys. Rev. B **67**, 035109 (2003).
[13]S. E. Tsimring, *Electron Beams and Microwave Vacuum Electronics* (John Wiley & Sons, Hoboken, NJ, 2007).
[14]D. M. Goebel *et al.*, IEEE Trans. Plasma Sci. **22**, 547 (1994).
[15]R. Marques, L. Jelinek, F. Mesa, and F. Medina, Opt. Express **17**, 11582 (2009).
[16]L. Jelinek, R. Marques, and J. Machac, Opt. Express **18**, 17940 (2010).
[17]C. Fietz, Y. Urzhumov, and G. Shvets, Opt. Express **19**, 19027 (2011).
[18]H.-T. Chen, W. J. Padilla, J. M. O. Zide, S. R. Bank, A. C. Gossard, A. J. Taylor, and R. D. Averitt, Nature **444**, 597 (2006).
[19]Y. P. Bliokh, S. Savel'ev, and F. Nori, Phys. Rev. Lett. **100**, 244803 (2008).
[20]RF Module, Comsol Inc. [www.comsol.com].
[21]R. Marques, F. Medina, and R. Rafii-El-Idrissi, Phys. Rev. B **65**, 144440 (2002).
[22]Z. Li, K. Aydin, and E. Ozbay, Phys. Rev. E **79**, 026610 (2009).
[23]W. Rotman, IRE Trans. Antennas Propag. **10**, 82 (1962).
[24]M. G. Silveirinha, A. Alù, and N. Engheta, Phys. Rev. E **75**, 036603 (2007).
[25]Y. A. Urzhumov and G. Shvets, Solid State Commun. **146**, 208 (2008).
[26]A. Fang, Th. Koschny, M. Wegener, and C. M. Soukoulis, Phys. Rev. B **79**, 241104(R) (2009).
[27]V. E. Semenov, E. I. Rakova, D. Anderson, M. Lisak, and J. Puech, IEEE Trans. Plasma Sci. **37**, 1774 (2009).